Co-expression of *SLC20A1* and *ALDH1A3* is associated with poor prognosis, and *SLC20A1* is required for the survival of ALDH1-positive pancreatic cancer stem cells

IZUMI MATSUOKA[1], TAKAHIRO KASAI[1], CHOTARO ONAGA[1], AYAKA OZAKI[1], HITOMI MOTOMURA[1], YUKI MAEMURA[1], YUNA TADA[1], HARUKA MORI[1], YASUSHI HARA[2], YUYUN XIONG[1], KEIKO SATO[3,4], SHOMA TAMORI[1,3], KAZUNORI SASAKI[5], SHIGEO OHNO[5] and KAZUNORI AKIMOTO[1,3]

[1]Department of Medicinal and Life Sciences, Faculty of Pharmaceutical Sciences, Tokyo University of Science, Noda, Chiba 278-8510, Japan; [2]Research Institute for Biomedical Sciences, Tokyo University of Science, Noda, Chiba 278-8510, Japan; [3]Research Division of Medical Data Science, Research Institute for Science and Technology, Tokyo University of Science, Noda, Chiba 278-8510, Japan; [4]Department of Information Sciences, Faculty of Science and Technology, Tokyo University of Science, Noda, Chiba 278-8510, Japan; [5]Laboratory of Cancer Biology, Institute for Diseases of Old Age, Juntendo University School of Medicine, Tokyo 113-8421, Japan

Abstract. Solute carrier family 20 member 1 (SLC20A1) is a sodium/inorganic phosphate symporter, which has been identified as a prognostic marker in several types of cancer, including pancreatic cancer. However, to the best of our knowledge, the association between *SLC20A1* expression and cancer stem cell (CSC) markers, such as aldehyde dehydrogenase 1 (ALDH1), in pancreatic ductal adenocarcinoma (PDAC), and the role of *SLC20A1* in PDAC CSCs remains unclear. In the present study, a genomic dataset of primary pancreatic cancer (The Cancer Genome Atlas, Pan-Cancer Atlas) was downloaded and analyzed. Kaplan-Meier analysis and multivariate Cox regression analysis were performed to evaluate the overall survival, disease-specific survival (DSS), disease-free interval (DFI) and progression-free interval (PFI). Subsequently, *SLC20A1* small interfering RNA (siRNA) knockdown (KD) was induced in the PANC-1 and MIA-PaCa-2 PDAC cell lines, and in sorted high ALDH1 activity (ALDH1^{high}) cells, after which, cell viability, *in vitro* tumor sphere formation, cell death and caspase-3 activity were examined. The results revealed that patients with high expression of *SLC20A1* (*SLC20A1*^{high}) at tumor stage I had a poor prognosis compared with patients with low expression of *SLC20A1* (*SLC20A1*^{low}) in terms of DSS, DFI and PFI. In addition, patients with high expression of *SLC20A1* and *ALDH1A3* (*SLC20A1*^{high}*ALDH1A3*^{high}) exhibited poorer clinical outcomes than patients with high expression of *SLC20A1* and low expression of *ALDH1A3* (*SLC20A1*^{high}*ALDH1A3*^{low}), low expression of *SLC20A1* and high expression of *ALDH1A3* (*SLC20A1*^{low}*ALDH1A3*^{high}) and *SLC20A1*^{low}*ALDH1A3*^{low}. *SLC20A1* siRNA KD in ALDH1^{high} cells isolated from PANC-1 and MIA-PaCa-2 cell lines resulted in suppression of *in vitro* tumorsphere formation, and enhancement of cell death and caspase-3 activity. These results suggested that *SLC20A1* was involved in cell survival via the suppression of caspase-3-dependent apoptosis, and contributed to cancer progression and poor clinical outcomes in PDAC. In conclusion, *SLC20A1* may be used as a prognostic marker and novel therapeutic target of ALDH1-positive pancreatic CSCs.

Introduction

Pancreatic ductal adenocarcinoma (PDAC) is the seventh leading cause of cancer-associated mortality worldwide (1). Despite improvements in diagnostic and therapeutic methods, its 5-year survival rate remains ~10%, which is the lowest among all of the cancer types investigated in the USA (2). The reasons why patients with PDAC exhibit a poor prognosis include its rapid progression, limited medical treatments and low therapeutic effect. The majority of patients are diagnosed after invasion and distant metastasis (3-5), and are not candidates for surgical tumor resection, and it is thus difficult to cure completely. Therefore, it is important to develop a biomarker for early prognosis and targeted drugs for PDAC.

Cancer stem cells (CSCs) have stemness properties such as self-renewal, multipotency and the promotion of tumorigenesis (6,7). CSCs exhibit resistance to standard therapies, such as chemotherapy and radiotherapy, and therefore can cause

relapse after treatments (6-8). In PDAC, cells with high aldehyde dehydrogenase 1 (ALDH1) activity (ALDH1^{high}) have stemness properties, such as self-renewal, differentiation, and tumor formation (9-13). ALDH1 is a detoxification enzyme that converts aldehydes into carboxylic acids in cells, and has several subtypes, including ALDH1A1 and ALDH1A3, which are known as CSC markers in several types of cancer (9,14-16). It is known that ALDH1A1 and ALDH1A3 expression levels are higher in PDAC tumors than in normal tissues, and that high ALDH1A3 expression in PDACs is associated with poor clinical outcomes (17-19).

Solute carrier family 20 member 1 (SLC20A1) is a sodium/inorganic phosphate (Pi) symporter that is responsible for Pi uptake into cells (20,21). Previous reports have shown that high *SLC20A1* expression is a prognostic factor for esophageal carcinoma, and breast, lung, pancreatic and prostate cancers (22-31). At the early tumor stage of estrogen receptor-positive (ER[+]) breast cancer, high *SLC20A1* expression predicts a poor clinical outcome (22). Furthermore, high *SLC20A1* expression is less effective for endocrine therapy and predicts late recurrence in ER[+] breast cancer (22), and is also less effective for radiotherapy in basal-like, claudin-low and ER[+] subtypes of breast cancer (23,24). In addition, *SLC20A1* contributes to cell viability and tumor formation of ALDH1-positive breast CSCs (23). In HeLa, HepG2, MC3T3-E1 and NIH3T3 cell lines, *SLC20A1* small interfering RNA (siRNA) knockdown (KD) has been shown to induce the suppression of cell proliferation and cell motility, and to induce TNFα-mediated apoptosis (32-34). However, the relationship between *SLC20A1* expression and CSC markers, such as ALDH1, in PDAC, and the role of *SLC20A1* in PDAC CSCs remains to be elucidated.

This study revealed that high *SLC20A1* expression indicated a poor prognosis at the early tumor stage of PDAC, and high expression levels of *SLC20A1* and *ALDH1A3* indicated a poorer prognosis in PDAC. In addition, the current results showed that *SLC20A1* was involved in cell survival and the formation of tumorspheres in ALDH1-positive PDAC CSCs.

Materials and methods

Analysis of the pancreatic adenocarcinoma [The Cancer Genome Atlas (TCGA), Pan-Cancer Atlas)] dataset. The TCGA, Pan-Cancer Atlas dataset (n=184) (35,36) was downloaded from cBioPortal (https://www.cbioportal.org/) (37,38) on December 8, 2020. Data on *SLC20A1* expression in normal tissues and primary tumors that were not derived from the same patients were downloaded from UALCAN (39). Statistical analyses were carried out by BellCurve for Excel version 4.03 software (Social Survey Research Information Co., Ltd.). The clinicopathological data of the Pan-Cancer Atlas dataset are summarized in Table SI. TCGA, Pan-Cancer Atlas dataset contains data on gene alterations, mRNA expression levels of primary pancreatic cancer samples (n=177), overall survival (OS) (n=177), disease-specific survival (DSS) (n=171), disease-free interval (DFI) (n=69), progression-free interval (PFI) (n=177), gene mutation (n=172) and copy number alteration (n=176). Beeswarm plots were drawn in GraphPad Prism ver. 9.5.1 (GraphPad Software) and analyzed expression of *SLC20A1* gene in patients with gene

alternations. The optimal cutoff thresholds to classify the patients into high- and low-mRNA expression groups were defined using receiver operator characteristic curve (ROC) of *SLC20A1* and other stem cell markers, and was determined by using the Youden's index. Survival curves of OS, DSS, DFI and PFI were depicted using the Kaplan-Meier method, and were compared by log-rank (Cochran-Mantel-Haenszel) test. Multivariate Cox regression analysis with age at diagnosis and sex as confounding factors was performed to evaluate the influence of gene expression, and to estimate adjusted hazard ratios (HRs) for OS, DSS, DFI and PFI statuses. Two-sided P<0.05 was considered to indicate a statistically significant difference.

Cell lines and culture. The human PDAC cell line PANC-1 was purchased from the American Type Culture Collection (CRL-1469; Manassas, Virginia, USA). The MIA-PaCa-2 cell line was purchased from the Japanese Cancer Research Resources Bank (JCRB0070; Tokyo, Japan). Both cell lines were cultured in Dulbecco's Modified Eagle Medium (DMEM) containing 10% fetal bovine serum (cat. no. 175012; Nichirei Biosciences, Inc.), L-glutamine (cat. no. 073-05391; Wako, Tokyo, Japan) and 1% penicillin/streptomycin (cat. no. 168-23191; Wako) at 37°C with 5% CO_2. These cell lines were evaluated by using a mycoplasma detecting kit (cat. no. 25235; Intron Biotechnology, Inc.) and were negative for mycoplasma.

siRNA transfection. RNA interference-mediated *SLC20A1* KD was performed by transfection of the PDAC cell lines with Dicer-Substrate Short Interfering RNA (DsiRNA) for *SLC20A1* (sense strand, 5'-CUCUAGUGGCUUCAGUAU UGAACTG-3'; antisense strand, 5'-CAGUUCAAUACUGAA GCCACUAGAGGG-3') (Integrated DNA Technologies, Inc., Iowa, USA) (23). Control DsiRNA (sense strand, 5'-CGUUAA UCGCGUAUAAUACGCGUAT-3'; antisense strand, 5'-AUA CGCGUAUUAUACGCGAUUAACGAC-3') (Integrated DNA Technologies, Inc., Iowa, USA) was used as a negative control (NC). Transfection was performed using Lipofectamine® RNAiMAX (cat. no. 13778-150; Thermo Fisher Scientific, Inc.). Cells were transfected with 10 nM DsiRNA and incubated for 24 h, followed by re-transfection with 10 nM DsiRNA and incubation for an additional 24 h, and were then subjected to assays. KD efficiency was monitored by quantitative PCR (qPCR) as detailed in the next section. In the tumorsphere formation, WST-8 assay, trypan-blue assay, caspase-3/7 fluorometric assay, and apoptosis staining, qPCR of *SLC20A1* was performed 48 h after first DsiRNA transfection. In the western blot analysis of proteins associated with p38, JNK, p44/42 and Akt signaling, 48 h after DsiRNA transfection, the subsequent tumorspheres were cultured for 72 h (PANC-1) or 24 h (MIA-PaCa-2), and then qPCR were done.

qPCR. qPCR was conducted as previously described (17,23,40). mRNA expression was examined with THUNDERBIRD probe qPCR Mix (TOYOBO) according to the manufacturer's instructions. The reaction conditions were as follows: 95°C for 1 min, followed by 45 cycles of denaturation at 95°C for 10 sec and extension at 60°C for 1 min. The following probes were used: *SLC20A1* probe, 5'-/FAM/TTAGGCAACTGC

ACTGCACCATTCACGG/TAMRA/-3'; forward primer, 5'-GCGTGGACTTGAAAGAGGAAAC-3'; and reverse primer, 5'-CTGACGGCTTGACTGAACTGG-3'; ALDH1A1 probe, 5'-/6-FAM/TGGAAGAGA/ZEN/ACTGGGAGAGTA CGGTT/3IABkFQ/-3'; forward primer, 5'-GTTCTTCTGAGA GATTTTCACTGTG-3'; and reverse primer, 5'-TGGTGGATT CAAGATGTCTGG-3' and ALDH1A3 probe, 5'-/6-FAM/ AGATAAGCC/ZEN/CGACGTGGACAAGG/3IABkFQ/-3'; forward primer, 5'-CTCTGGAAGGCAACCTGTG-3'; and reverse primer, 5'-GGAGCAAATATGTGAAGTGGA AG-3'. Quantification was performed using the calibration curve method (17,23,40). We used the Eukaryotic 18S rRNA Endogenous Control (4319413E; Thermo Fisher Scientific, Inc.) and normalization was performed based on the internal control. The sequences were not disclosed.

Tumorsphere culture. *In vitro* tumorsphere formation was carried out as previously described (10,23,40-43). After *SLC20A1* KD, unsorted cells and isolated ALDH1^{high} cells were seeded in ultralow attachment 96-well plates (1x10^3 cells/ well) (cat. no. 655970; Greiner Bio-One GmbH) and cultured for 5 days in medium containing 0.6% methylcellulose (cat. no. 22222-62; Nacalai Tesque, Inc., Kyoto, Japan). Images were captured using a microscope (DM5500B; Leica Microsystems, Inc.). The number and size of tumorspheres >314 μm^2 were calibrated using ImageJ 1.51j8; Java 1.8.0_112 [64-bit] software (National Institutes of Health, Bethesda, Maryland, USA).

WST-8 assay. The WST-8 assay was performed as previously described (10,40,44,45). After *SLC20A1* KD, unsorted and sorted ALDH1^{high} cells were plated into 96-well plates (1x10^3 cells/well) (cat. no. 167008, Thermo Fisher Scientific, Inc.) and were incubated for 5 days. A color reaction was carried out using Cell Counting Reagent SF (cat. no. 07553-44, Nacalai Tesque, Inc.) and the formed formazan dye was measured using a Sunrise Remote microplate reader (Tecan Group, Ltd.) at 450 nm.

Trypan blue assay. The trypan blue assay was carried out as previously described (40,44). Unsorted and sorted ALDH1^{high} cells were plated into 12-well plates (cat. no. 150628; Thermo Fisher Scientific, Inc.) at a density of 2x10^4 cells per well in the case of unsorted cells or 1.5x10^4 cells per well for sorted ALDH1^{high} cells. After 48 h of incubation, cells were stained with 0.4% w/v trypan blue solution (cat. no. 207-17081; Wako, Tokyo, Japan) and trypan blue-positive cells were counted using a hemocytometer (cat. no. 03-202-1; Erma Inc.).

Caspase-3/7 fluorometric assay. The Apo-ONE® Homogeneous Caspase-3/7 Assay kit (cat. no. G7790; Promega Corporation) was used as previously described (40,44). Unsorted and sorted ALDH1^{high} cells were plated into 96-well black plates (cat. no. 3916; Corning, Inc.) at a density of 1x10^4 cells per well, and were incubated for 48 h (unsorted cells) or 24 h (sorted ALDH1^{high} cells). Apo-ONE® caspase reagent was then added to the cells, and the mixture was incubated for 30 min at room temperature. Fluorescence was measured using a fluorescence plate reader (excitation, 485 nm; emission, 535 nm) (ARVO; PerkinElmer, Inc.). The background fluorescence was measured as the fluorescence from DMEM alone and was subtracted from all of the experimental values.

Western blotting. PANC-1 and MIA-PaCa-2 cells from two-dimensional monolayer culture or three-dimensional tumorspheres were lysed in RIPA buffer containing a protease inhibitor (cat. no. 03969-21, Nacalai Tesque, Inc.) and a phosphatase inhibitor (cat. no. 07575-51; Nacalai Tesque, Inc.). Western blotting was carried out as previously described (40,44,45). Extracts were then separated by SDS-PAGE on 8% gels and were transferred onto Immobilon-P membranes (cat. no. ISEQ00010; MilliporeSigma). The membranes were then blocked with 5% skim milk or BSA in TBS-Tween 20, incubated with primary antibodies at 4˚C for 18 h, and then probed with horseradish peroxidase-conjugated secondary antibodies. Specific signals were detected using the chemiluminescence reagents Immunostar LD (cat. no. 290-69904; Wako) or EzWestLumiOne (cat. no. 2332632; ATTO Corporation, Tokyo, Japan) with ChemiDoc MP (Bio-Rad Laboratories, Inc.). The primary antibodies were as follows: mouse anti-p-p38 monoclonal antibody (mAb) (cat. no. 9216s; Cell Signaling Technology, Inc.; 1:3,000); rabbit anti-p38 polyclonal antibody (pAb) (cat. no. 9212s; Cell Signaling Technology, Inc. Danvers, MA, USA; 1:3,000); rabbit anti-phosphorylated (p)-c-Jun N-terminal Kinase (JNK) pAb (cat. no. 9251s; Cell Signaling Technology, Inc.; 1:3,000); rabbit anti-JNK pAb (cat. no. 9252s; Cell Signaling Technology, Inc.; 1:3,000); rabbit anti-p-p44/p42 pAb (cat. no. 9101s; Cell Signaling Technology, Inc.; 1:3,000); rabbit anti-p44/p42 pAb (cat. no. 9102s; Cell Signaling Technology, Inc.; 1:3,000); rabbit anti-p-Akt S473 mAb (cat. no. 4060s; Cell Signaling Technology, Inc.; 1:3,000); rabbit anti-Akt mAb (cat. no. 2938s; Cell Signaling Technology, Inc.; 1:3,000); rabbit anti-ALDH1A1 mAb (cat. no. ab52492; Abcam; 1:5,000); rabbit anti-ALDH1A3 pAb (cat. no. PA5-29188; Thermo Fisher Scientific, Inc.; 1:5,000); and mouse anti-β-actin mAb (cat. no. 60008-1-Ig; ProteinTech Group, Inc.; 1:10,000). Goat anti-mouse and anti-rabbit IgG (cat. no. 7076S and 7074S, respectively; Cell Signaling Technology, Inc.) were used as secondary antibodies according to the primary antibody used. β-actin as the internal control was reprobed with mouse anti-β-actin mAb after stripping targeted antibody. Stripping was performed using Stripping solution (cat. no. 193-16375, Wako) according to the manufacturer's protocol.

ALDEFLUOR assay. ALDH1^{high} cells were isolated from the PANC-1 and MIA-PaCa-2 cell lines using the ALDEFLUOR™ assay kit (cat. no. ST-01700; Stemcell Technologies, Inc., Vancouver, BC, Canada) according to the manufacturer's protocol as previously described (10,40,44). The cell population with the highest ALDH1 activity (5-10% of total cells) was sorted as ALDH1^{high} cells by the FACS Aria III or FACS Melody cell sorters (BD Biosciences), whereas the cell population with the lowest ALDH1 activity was sorted as ALDH1^{low} cells.

Apoptosis staining. Apoptotic staining of ALDH1^{high} PANC-1 and ALDH1^{high} MIA-PaCa-2 cells was performed using the Cell Meter™ Apoptotic and Necrotic Multiplexing Detection Kit I (cat. no. 22840; AAT Bioquest, Inc.) according to the manufacturer's

protocol. Living cells were stained with 0.1% Hoechst 33342 (cat. no. H3570; Invitrogen; Thermo Fisher Scientific, Inc.). Images were then captured using a microscope (DMI6000B-AFC; Leica Corporation) and the number of stained cells was counted with the counting software Katikaticounter (Vector Laboratories, Inc.).

Statistical analysis. For the gene expression analysis, to analyze *SLC20A1* expression in normal tissues and primary tumors using the downloaded data from UALCAN, P-values were calculated using an unpaired Student's t-test. P-values for the comparisons of gene expression among stages were calculated using the Kruskal-Wallis test with Steel's post hoc test. Pearson's correlation coefficients (r) were calculated and P-values were calculated using the t-test for testing the population correlation coefficient is zero (null hypothesis). To analyze the association between gene expression of CSC markers such as *SLC20A1*, *ALDH1A1* and *ALDH1A3*, and gene mutation or copy number alterations of *KRAS*, *CDKN2A*, *TP53* and *SMAD4*, P-values were calculated using the Kruskal-Wallis test with Steel's test. Survival curves were plotted by the Kaplan-Meier method for univariate analysis, and P-values were calculated by the Cochran-Mantel-Haenszel generalized log-rank test. Multiplicity was adjusted using the Bonferroni test as a post hoc test. A multivariate Cox regression model with age and sex as a confounding factor was performed to evaluate the effect of gene expression and to estimate the adjusted HRs. Statistical analysis was performed using BellCurve for Excel version 4.04 software (Social Survey Research Information Co., Ltd.). Tumorsphere formation data and the relative number of apoptotic cells are shown as the mean ± standard deviation of three independent experiments, whereas data obtained from the WST-8, trypan blue and caspase-3/7 fluorometric assays are shown as the mean ± standard error (SE) of three independent experiments and were analyzed using an unpaired Student's t-test. To examine the siRNA knockdown efficiency, the statistical significance between NC KD and *SLC20A1* KD cells was determined using an unpaired Student's t-test. Two-sided P<0.05 was considered to indicate a statistically significant difference. For the mRNA expression analysis in ALDH1high and ALDH1low MIA-PaCa-2 cells, data are shown as the mean ± SE of three independent experiments and were analyzed using an unpaired Student's t-test.

Results

High SLC20A1 gene expression is associated with driver gene mutation for KRAS, CDKN2A, TP53 and SMAD4 in PDAC. Our group previously reported that *SLC20A1* gene expression was higher in breast cancer than in normal breast tissues (23). The present study explored *SLC20A1* expression in PDAC. Unlike breast cancer, *SLC20A1* gene expression was not statistically significantly different in PDAC tumors compared to normal tissues (Fig. S1A). Next, *SLC20A1* expression was compared according to tumor stages. Although *SLC20A1* expression was largely unchanged between normal tissues and stage I tumors, the expression of *SLC20A1* gradually increased in the order of stage II, III and IV compared with stage I (Fig. S1B). A similar expression pattern of *SLC20A1* was obtained from another dataset (Fig. S1C). There was no gene amplification, deletion or fusion, and only 1 patient with

Table I. Multivariate Cox regression analyses of differences in OS, DSS, DFI and PFI between *SLC20A1*high and *SLC20A1*low groups of patients with pancreatic cancer at tumor stages I, II and III/IV.

Survival status	Hazard ratio	95% confidence interval	P-value
OS	2.20	1.16-4.15	0.02
DSS	2.72	1.29-5.73	<0.01
DFI	4.08	1.52-10.98	<0.01
PFI	2.33	1.34-4.06	<0.01
Staging (OS)			
Stage I	6.39	0.60-67.61	0.12
Stage II	1.16	0.72-1.86	0.55
Stage III/IV		N.D.	
Staging (DSS)			
Stage I		N.D.	
Stage II	1.93	1.07-3.48	0.03
Stage III/IV		N.D.	
Staging (DFI)			
Stage I		N.D.	
Stage II	3.33	0.97-11.41	0.06
Stage III/IV		N.D.	
Staging (PFI)			
Stage I		N.D.	
Stage II	1.81	1.10-2.97	0.02
Stage III/IV	10.10	1.42-71.68	0.02

The Cancer Genome Atlas Pan-Cancer data were downloaded from cBioPortal. Hazard ratio: Hazard ratio of the *SLC20A1*high group relative to the *SLC20A1*low group adjusted using age and sex as a confounding factor as estimated using a Cox proportional hazard model. OS, overall survival; DSS, disease-specific survival; DFI, disease-free interval; PFI, progression-free interval; *SLC20A1*, solute carrier family 20 member 1; *SLC20A1*high, high *SLC20A1* expression; *SLC20A1*low, low *SLC20A1* expression; N.D., not determined.

PDAC had a mutation in the *SLC20A1* locus (0.57%, 1/175). In PDAC progression, a multistep carcinogenesis proceeds from sequential mutations in driver genes for *KRAS*, *CDKN2A*, *TP53*, and *SMAD4* in the premalignant state (46). Therefore, we next examined whether these driver gene mutations were associated with *SLC20A1* gene expression (Fig. 1). *SLC20A1* gene expression in PDAC tumors with *KRAS* missense mutations, such as G12D, G12V, G12R and G12C, was significantly higher than that in PDAC tumors without *KRAS* mutations (Fig. 1A). *TP53* missense and truncating mutations were also associated with high *SLC20A1* expression (Fig. 1C). In addition, *SLC20A1* expression in PDAC tumors with deep deletion and deletion of *CDKN2A*, *TP53*, or *SMAD4* was higher than that with each diploid gene (Fig. 1F-H). *KRAS* missense mutations are introduced during the early steps of premalignant progression in PDAC. Therefore, these results suggested that high *SLC20A1* expression may be obtained during an early step of PDAC progression.
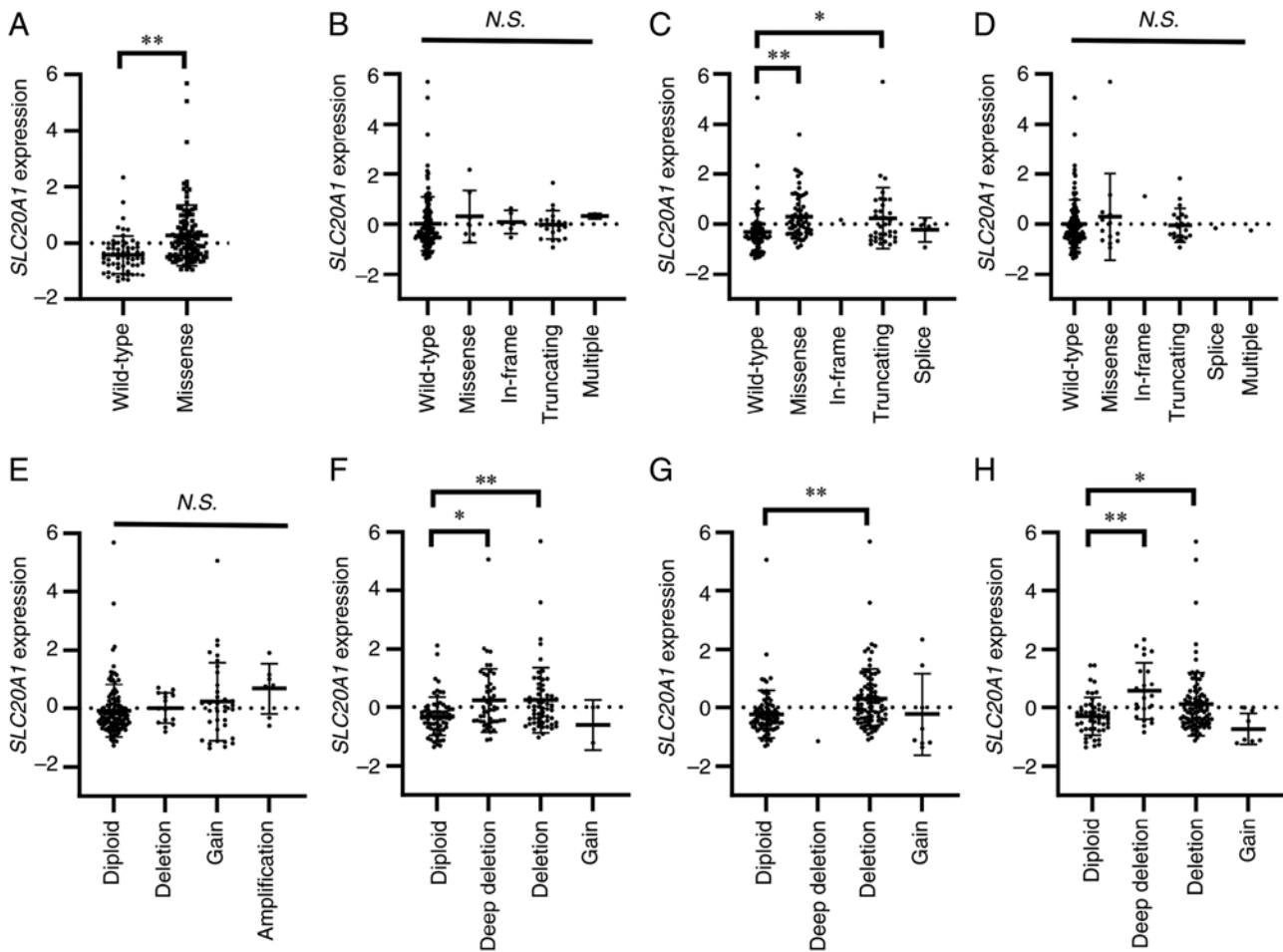
Figure 1. Association between *SLC20A1* gene expression and gene mutation or copy number alterations of *KRAS*, *CDKN2A*, *TP53* and *SMAD4*. (A-H) Beeswarm plots showing the association between *SLC20A1* gene expression and driver gene status. (A-D) Comparison of *SLC20A1* gene expression and gene mutations (wild-type, missense, in-frame, truncating, splice and multiple) of (A) *KRAS*, (B) *CDKN2A*, (C) *TP53* and (D) *SMAD4*. (E-H) Comparison of *SLC20A1* gene expression and copy number alterations of (E) *KRAS*, (F) *CDKN2A*, (G) *TP53* and (H) *SMAD4*. *P<0.05, **P<0.01; Kruskal-Wallis test with Steel's test. *SLC20A1*, solute carrier family 20 member 1; *KRAS*, KRAS proto-oncogene, GTPase; *CDKN2A*, cyclin dependent kinase inhibitor 2A; *TP53*, tumor protein p53; *SMAD4*, SMAD family member 4; *N.S.*, not significant.

Patients with SLC20A1^{high} at stage I have a poorer prognosis. To examine the association between *SLC20A1* gene expression and the prognosis of different tumor stages, as indicated by parameters such as OS, DSS, DFI and PFI, Kaplan-Meier and multivariate Cox regression analyses were performed. Kaplan-Meier analyses of all tumors indicated that patients with *SLC20A1*^{high} showed poorer prognoses than patients with *SLC20A1*^{low} (OS: P=0.0080; DSS: P=0.0050; DFI: P=0.011; and PFI: P=0.0023) (Fig. 2A-D). Kaplan-Meier analyses at tumor stage I indicated that patients with *SLC20A1*^{high} showed poorer prognosis than those with *SLC20A1*^{low} (DSS: P=0.017; DFI: P<0.001; and PFI: P<0.001) (Fig. 2E-H). At tumor stage II, Kaplan-Meier analyses comparing OS, DSS and DFI did not show significant differences between patients with *SLC20A1*^{high} or *SLC20A1*^{low} (Fig. 2I-K). However, patients with *SLC20A1*^{high} showed poorer prognosis than patients with *SLC20A1*^{low} regarding PFI (P=0.026) (Fig. 2L). At tumor stages III and IV, there was no significant differences between patients with *SLC20A1*^{high} or *SLC20A1*^{low} regarding OS, DSS or PFI (Fig. 2M-O). Notably, DFI data were not available as there were not enough patients for analysis. Multivariate Cox regression analysis of all patients with age at diagnosis and sex as confounding factors also showed that patients with *SLC20A1*^{high} had poor clinical outcomes [OS: HR=2.20, 95% confidence interval (CI)=1.16-4.15, DSS: HR=2.72, 95% confidence interval (CI)=1.29-5.73; DFI: HR=4.08, 95% CI=1.52-10.98; and PFI: HR=2.33, 95% CI=1.34-4.06] (Table I). At tumor stage II, patients with *SLC20A1*^{high} showed poor clinical outcome (stage II: HR=1.93, 95% CI=1.07-3.48), but DSS could not be evaluated at stage I, III or IV. In terms of PFI, patients with *SLC20A1*^{high} at stage II, III and IV had poor prognosis (stage II: HR=1.81, 95% CI=1.10-2.97; stage III and IV: HR=10.10, 95% CI=1.42-71.68) (Table I). These results also suggested that *SLC20A1* was involved in cancer progression at an early stage and high expression of *SLC20A1* was associated with poor prognosis in PDAC.

SLC20A1 siRNA KD suppresses in vitro tumorsphere formation and cell viability, and increases cell death and caspase-3 activity. To investigate the roles of *SLC20A1* in PDAC cells, the present study next examined the effects of *in vitro* loss of function via siRNA KD on tumor formation, cell viability and cell death using two PDAC cell lines expressing *SLC20A1*, namely PANC-1 and MIA-PaCa-2.
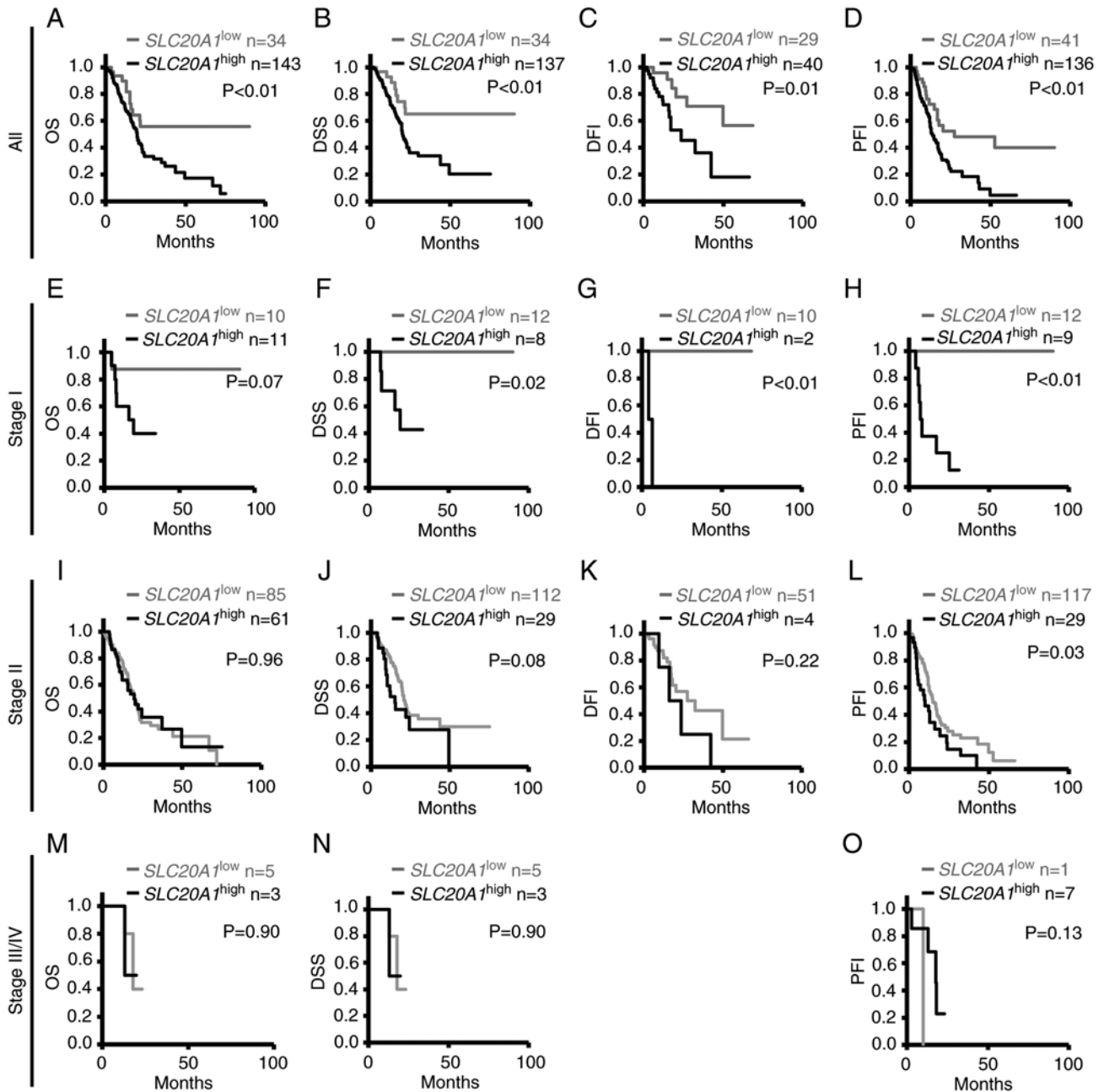
Figure 2. Kaplan-Meier analyses of differences in OS, DSS, DFI and PFI between *SLC20A1*high and *SLC20A1*low groups of patients in pancreatic cancer at tumor stages I, II and III/IV. The Cancer Genome Atlas Pan-Cancer data were downloaded from cBioPortal. (A-D) All patients with pancreatic cancer: (A) OS, (B) DSS, (C) DFI and (D) PFI. (E-H) Patients at stage I: (E) OS, (F) DSS, (G) DFI and (H) PFI. (I-L) Patients at stage II: (I) OS, (J) DSS, (K) DFI and (L) PFI. (M-O) Patients at stage III/IV: (M) OS, (N) DSS and (O) PFI. DFI data were not available as there were not enough patients for analysis. (M and N) For DSS and OS analysis, the same patients were included in the *SLC20A1*high and *SLC20A1*low groups. P-values were calculated by the Cochran-Mantel-Haenszel generalized log-rank test. OS, overall survival; DSS, disease-specific survival; DFI, disease-free interval; PFI, progression-free interval; *SLC20A1*, solute carrier family 20 member 1; *SLC20A1*high, patients with high expression of *SLC20A1*; *SLC20A1*low, patients with low expression of *SLC20A1*.

The results of the *in vitro* tumorsphere formation assay revealed that *SLC20A1* siRNA KD in PANC-1 and MIA-PaCa-2 resulted in the suppression of tumorsphere formation in comparison with NC siRNA KD cells (Fig. 3A and B). In addition, *SLC20A1* siRNA KD suppressed the viability of both PDAC cell lines (Fig. 3C and D).

A previous study has shown that *SLC20A1* deficiency causes the promotion of caspase-3-dependent apoptosis in HeLa cells stimulated with TNFα (32). Therefore, the current study next examined apoptosis in these PDAC cell lines via trypan blue dye exclusion assay and caspase-3/7 activity analysis. As

shown in Fig. 3E-H, *SLC20A1* siRNA KD induced an increase in the number of trypan blue-positive cells (Fig. 3E and F) and enhanced caspase-3/7 activity (Fig. 3G and H). When the activity of the MAPK family and its downstream Akt protein was examined, *SLC20A1* deficiency was found to result in the enhancement of the phosphorylation levels of p38 kinase and Akt, but not ERK and JNK (Fig. 4A-S). Thus, *SLC20A1* may suppress p38 stress kinase-dependent cell death. Moreover, these results suggested that *SLC20A1* was required for cell survival and tumorsphere formation via suppressing caspase-3-dependent apoptosis in PDAC cells.
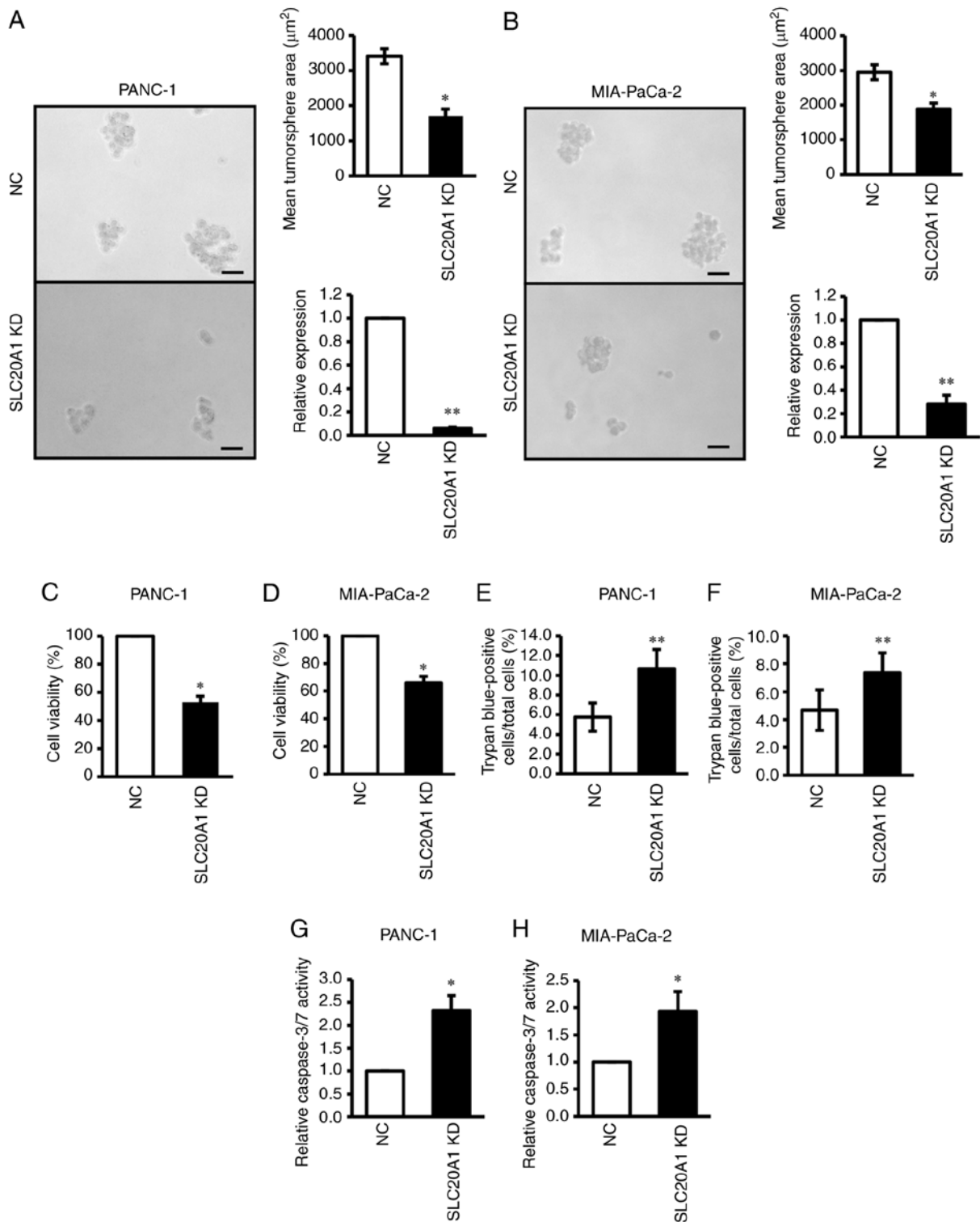
Figure 3. Effects of *SLC20A1* small interfering RNA KD on the tumorsphere formation, viability, cell death and apoptosis of pancreatic cancer cell lines. (A and B) Representative images, mean tumorsphere area (μm) and relative *SLC20A1* mRNA expression following transfection with *SLC20A1* siRNA or NC siRNA in (A) PANC-1 and (B) MIA-PaCa-2 cells. Scale bar, 50 μm. Viability of (C) PANC-1 and (D) MIA-PaCa-2 cells was assessed using 5-{2,4-bis[(sodiooxy) sulfonyl]phenyl}-2-(2-methoxy-4-nitrophenyl)-3-(4-nitrophenyl)-3H-1,2λ5,3,4-tetrazol-2-ylium assays. Trypan blue-positive (E) PANC-1 and (F) MIA-PaCa-2 cells. The total cells and the stained cells were counted using a hemocytometer and the percentage of the stained cells per total cells was calculated. Relative caspase-3/7 activity of (G) PANC-1 and (H) MIA-PaCa-2 cells, as assessed by a caspase-3/7 fluorometric assay. *P<0.05, **P<0.01 vs. NC; unpaired Student's t-test. *SLC20A1*, solute carrier family 20 member 1; NC, negative control; KD, knockdown; siRNA, small interfering RNA.

Patients with PDAC SLC20A1^high ALDH1A3^high have a poor prognosis. SLC20A1 is known to be involved in cell viability and *in vitro* tumorsphere formation of ALDH1-positive breast CSCs (23); however, the roles of *SLC20A1* in PDAC CSCs

remain unclear. Therefore, the association between *SLC20A1* gene expression and various stem cell markers, including *ALDH1A1* and *ALDH1A3*, was examined. As shown in Fig. S2, *SLC20A1* gene expression was positively correlated

Table II. Multivariate Cox regression analyses of differences in DSS, DFI and PFI between groups based on *SLC20A1* and CSC marker expression.

Survival status	Hazard ratio	95% confidence interval	P-value
DSS: *SLC20A1*^{high}*ALDH1A1*^{high} vs.			
SLC20A1^{high}*ALDH1A1*^{low}	0.90	0.49-1.63	0.72
SLC20A1^{low}*ALDH1A1*^{high}	3.00	0.96-9.41	0.06
SLC20A1^{low}*ALDH1A1*^{low}	1.66	0.53-5.24	0.39
DSS: *SLC20A1*^{high}*ALDH1A3*^{high} vs.			
SLC20A1^{high}*ALDH1A3*^{low}	1.47	0.88-2.44	0.14
SLC20A1^{low}*ALDH1A3*^{high}		N.D.	
SLC20A1^{low}*ALDH1A3*^{low}	3.65	1.63-8.20	<0.01
DSS: *SLC20A1*^{high}*CD44*^{high} vs.			
SLC20A1^{high}*CD44*^{low}	1.62	0.80-3.28	0.18
SLC20A1^{low}*CD44*^{high}	1.82	0.66-5.04	0.25
SLC20A1^{low}*CD44*^{low}	4.11	1.46-11.59	<0.01
DSS: *SLC20A1*^{high}*CD133*^{high} vs.			
SLC20A1^{high}*CD133*^{low}	1.48	0.70-3.12	0.30
SLC20A1^{low}*CD133*^{high}	1.56	0.74-3.32	0.25
SLC20A1^{low}*CD133*^{low}		N.D.	
DSS: *SLC20A1*^{high}*BMI1*^{high} vs.			
SLC20A1^{high}*BMI1*^{low}	0.70	0.40-1.22	0.21
SLC20A1^{low}*BMI1*^{high}	3.46	1.23-9.70	0.02
SLC20A1^{low}*BMI1*^{low}	1.78	0.61-5.17	0.29
DSS: *SLC20A1*^{high}*HIF1A*^{high} vs.			
SLC20A1^{high}*HIF1A*^{low}	1.52	0.91-2.54	0.11
SLC20A1^{low}*HIF1A*^{high}		N.D.	
SLC20A1^{low}*HIF1A*^{low}	3.47	1.49-8.10	<0.01
DSS: *SLC20A1*^{high} *KLF4*^{high} vs.			
SLC20A1^{high}*KLF4*^{low}	1.87	0.75-4.69	0.18
SLC20A1^{low}*KLF4*^{high}	1.71	0.73-3.99	0.21
SLC20A1^{low}*KLF4*^{low}	5.04	1.91-13.30	<0.01
DSS: *SLC20A1*^{high}*MET*^{high} vs.			
SLC20A1^{high}*MET*^{low}	2.55	1.46-4.44	<0.01
SLC20A1^{low}*MET*^{high}	1.70	0.71-4.06	0.23
SLC20A1^{low}*MET*^{low}	10.51	2.49-44.31	<0.01
DSS: *SLC20A1*^{high}*MYC*^{high} vs.			
SLC20A1^{high}*MYC*^{low}	1.73	0.95-3.12	0.07
SLC20A1^{low}*MYC*^{high}	1.65	0.69-3.94	0.26
SLC20A1^{low}*MYC*^{low}	7.86	1.87-32.95	<0.01
DSS: *SLC20A1*^{high}*NANOG*^{high} vs.			
SLC20A1^{high}*NANOG*^{low}	0.90	0.44-1.83	0.77
SLC20A1^{low}*NANOG*^{high}	0.17	0.25-0.21	0.18
SLC20A1^{low}*NANOG*^{low}	1.90	0.65-5.55	0.24
DSS: *SLC20A1*^{high}*NOTCH1*^{high} vs.			
SLC20A1^{high}*NOTCH1*^{low}	0.60	0.35-1.04	0.07
SLC20A1^{low}*NOTCH1*^{high}	2.54	0.33-19.74	0.37
SLC20A1^{low}*NOTCH1*^{low}	1.74	0.71-4.27	0.22
DSS: *SLC20A1*^{high}*NOTCH3*^{high} vs.			
SLC20A1^{high}*NOTCH3*^{low}	1.39	0.66-2.93	0.39
SLC20A1^{low}*NOTCH3*^{high}	1.89	0.75-4.80	0.18
SLC20A1^{low}*NOTCH3*^{low}	4.93	1.52-15.94	<0.01

Table II. Continued.

Survival status	Hazard ratio	95% confidence interval	P-value
DSS: $SLC20A1^{high}POU5F1^{high}$ vs.			
$SLC20A1^{high}POU5F1^{low}$	0.70	0.41-1.21	0.20
$SLC20A1^{low}POU5F1^{high}$	1.91	0.44-8.23	0.39
$SLC20A1^{low}POU5F1^{low}$	2.07	0.82-5.22	0.12
DSS: $SLC20A1^{high}SOX2^{high}$ vs.			
$SLC20A1^{high} SOX2^{low}$	0.63	0.33-1.18	0.15
$SLC20A1^{low} SOX2^{high}$	1.27	0.36-4.56	0.71
$SLC20A1^{low} SOX2^{low}$	1.85	0.63-5.46	0.26
DSS: $SLC20A1^{high}STAT3^{high}$ vs.			
$SLC20A1^{high}STAT3^{low}$	1.61	0.95-2.73	0.08
$SLC20A1^{low}STAT3^{high}$	3.89	0.82-18.40	0.09
$SLC20A1^{low}STAT3^{low}$	5.04	1.91-13.30	<0.01
DFI: $SLC20A1^{high}ALDH1A3^{high}$ vs.			
$SLC20A1^{high}ALDH1A3^{low}$	3.18	0.67-15.07	0.15
$SLC20A1^{low}ALDH1A3^{high}$	5.66	1.75-18.28	<0.01
$SLC20A1^{low}ALDH1A3^{low}$	54.54	5.66-525.68	<0.01
PFI: $SLC20A1^{high}ALDH1A3^{high}$ vs.			
$SLC20A1^{high}ALDH1A3^{low}$	1.43	0.79-2.58	0.23
$SLC20A1^{low}ALDH1A3^{high}$	1.42	0.69-2.89	0.34
$SLC20A1^{low}ALDH1A3^{low}$	4.37	1.82-10.51	<0.01

The Cancer Genome Atlas Pan-Cancer data were downloaded from cBioPortal. Hazard ratio: Hazard ratio of the high $SLC20A1$ and CSC markers expression ($SLC20A1^{high}$CSC marker^{high}) group relative to the $SLC20A1^{high}$CSC marker^{low}, $SLC20A1^{low}$CSC marker^{high} or $SLC20A1^{low}$CSC marker^{low} groups adjusted using age and sex as a confounding factor as estimated using a Cox proportional hazard model. The CSC markers were $ALDH1A1$, $ALDH1A3$, $CD44$, $CD133$, $BMI1$, $HIF1A$, $KLF4$, MET, MYC, $NANOG$, $NOTCH1$, $NOTCH3$, $POU5F1$, $SOX2$ and $STAT3$. CSC, cancer stem cell; DSS, disease-specific survival; DFI, disease-free interval; PFI, progression-free interval; $SLC20A1$, solute carrier family 20 member 1; $ALDH1A1$, aldehyde dehydrogenase 1 family member A1; $ALDH1A3$, aldehyde dehydrogenase 1 family member A3; $CD44$, CD44 molecule; $CD133$, prominin 1; $BMI1$, BMI1 proto-oncogene, polycomb ring finger; $HIF1A$, hypoxia inducible factor 1 subunit alpha; $KLF4$, KLF transcription factor 4; MET, MET proto-oncogene, receptor tyrosine kinase; MYC, MYC proto-oncogene, bHLH transcription factor; $NANOG$, Nanog homeobox; $NOTCH1$, notch receptor 1; $NOTCH3$, notch receptor 3; $POU5F1$, POU class 5 homeobox 1; $SOX2$, SRY-box transcription factor 2; $STAT3$, signal transducer and activator of transcription 3; $SLC20A1^{high}$CSC marker^{high}, patients with high expression of $SLC20A1$ and CSC marker; $SLC20A1^{low}$CSC marker^{low}, patients with low expression of $SLC20A1$ and CSC marker; $SLC20A1^{high}$CSC marker^{low}, patients with high expression of $SLC20A1$ and low expression of CSC marker; $SLC20A1^{low}$CSC marker^{high}, patients with low expression of $SLC20A1$ and high expression of CSC marker; N.D., not determined.

with stem cell markers, such as $KLF4$, MET, $NOTCH3$, $HIF1A$ and $CD44$, and tended to positively correlate with $ALDH1A3$, whereas $SLC20A1$ gene expression was negatively correlated with $ALDH1A1$.

Next, the association of $SLC20A1$ and stem cell markers with clinical outcomes was examined by Kaplan-Meier and multivariate Cox regression analyses. It is known that ALDH1A1, ALDH1A3, CD44 and CD133 are pancreatic CSC markers due to their properties of high tumorigenesis and therapy resistance (11-13,47-49). Therefore, the present study next examined the association between $SLC20A1$ and CSC markers, including the four aforementioned genes. First, patients were divided into four groups according to their expression levels of $SLC20A1$ and CSC markers: $SLC20A1^{high}$CSC marker^{high}, $SLC20A1^{high}$CSC marker^{low}, $SLC20A1^{low}$CSC marker^{high} and $SLC20A1^{low}$CSC marker^{low}. The prognosis in each group was then compared regarding OS and DSS (Kaplan-Meier analyses: Figs. 5A-D, S3A-H and S4A-K; Cox regression analyses: Tables II and III). In Kaplan-Meier curves, patients with

$SLC20A1^{high}ALDH1A3^{high}$ (red line) exhibited a significantly poor clinical outcome compared with the other three patient groups, $SLC20A1^{high}ALDH1A3^{low}$, $SLC20A1^{low}ALDH1A3^{high}$ and $SLC20A1^{low}ALDH1A3^{low}$ (Figs. 5B and S3F). On the other hand, patients with $SLC20A1^{high}ALDH1A1^{high}$ (Figs. 5A and S3E), $SLC20A1^{high}CD44^{high}$ (Figs. 5C and S3G) and $SLC20A1^{high}CD133^{high}$ (Figs. 5D and S3H) did not show a poorer outcome than others. As determined by Cox regression analyses, some CSC markers, such as $ALDH1A3$, $CD44$, $HIF1A$, $KLF4$, MET, MYC, $STAT3$ and $NOTCH3$, were associated with a significantly worse prognosis in the $SLC20A1^{high}$CSC marker^{high} group compared with the $SLC20A1^{low}$CSC marker^{low} group (Table II). Thus, the current study subsequently focused on $ALDH1A3$ as the CSC marker that may contribute with $SLC20A1$ to results in a poorer prognosis in PDAC.

In addition to OS and DSS-associated prognosis, the DFI and PFI of the aforementioned four groups divided according to $SLC20A1$ and $ALDH1A3$ were compared. Patients with

Table III. Cox regression analyses of OS in CSC marker[high] vs. CSC marker[low] patients and multivariate Cox regression analyses of differences in OS between groups based on *SLC20A1* and CSC marker expression.

OS	Hazard ratio	95% confidence interval	P-value
ALDH1A1^{high} vs. *ALDH1A1*^{low}	0.72	0.45-1.16	0.18
ALDH1A3^{high} vs. *ALDH1A3*^{low}	2.75	1.26-6.03	0.01
CD44^{high} vs. *CD44*^{low}	2.05	1.35-3.13	<0.01
CD133^{high} vs. *CD133*^{low}	3.09	1.42-6.75	<0.01
SLC20A1^{high}*ALDH1A1*^{high} vs.			
SLC20A1^{high}*ALDH1A1*^{low}	0.90	0.52-1.56	0.71
SLC20A1^{low}*ALDH1A1*[high]	1.83	0.74-4.45	0.19
SLC20A1[low]*ALDH1A1*[low]	1.77	0.58-5.45	0.32
SLC20A1[high]*ALDH1A3*[high] vs.			
SLC20A1[high]*ALDH1A3*[low]	1.48	0.46-4.72	0.51
SLC20A1[low]*ALDH1A3*[high]	1.32	0.61-2.88	0.48
SLC20A1[low]*ALDH1A3*[low]	4.19	1.51-11.64	<0.01
SLC20A1[high]*CD44*^{high} vs.			
SLC20A1[high]*CD44*^{low}	2.00	1.27-3.13	<0.01
SLC20A1[low]*CD44*^{high}	2.00	0.79-5.04	0.14
SLC20A1[low]*CD44*^{low}	3.56	1.51-8.42	<0.01
SLC20A1[high] *CD133*^{high} vs.			
SLC20A1[high]*CD133*^{low}	1.55	0.71-3.38	0.27
SLC20A1[low]*CD133*^{high}	1.23	0.65-2.33	0.52
SLC20A1[low]*CD133*^{low}		N.D.	

The CSC markers were *ALDH1A1*, *ALDH1A3*, *CD44* and *CD133*. OS, overall survival; *SLC20A1*, solute carrier family 20 member 1; *ALDH1A1*, aldehyde dehydrogenase 1 family member A1; *ALDH1A3*, aldehyde dehydrogenase 1 family member A3; *CD44*, CD44 molecule; *CD133*, prominin 1; CSC, cancer stem cell; *SLC20A1*[high]CSC marker[high], patients with high expression of *SLC20A1* and CSC marker; *SLC20A1*[low]CSC marker[low], patients with low expression of *SLC20A1* and CSC marker; *SLC20A1*[high]CSC marker[low], patients with high expression of *SLC20A1* and low expression of CSC marker; *SLC20A1*[low]CSC marker[high], patients with low expression of *SLC20A1* and high expression of CSC marker; N.D., not determined.

SLC20A1[high]*ALDH1A3*[high] showed a poorer clinical outcome than the other groups in terms of DFI (Fig. 5E) and PFI (Fig. 5F). Next, multivariate Cox regression analysis was conducted with confounding factors such as age at diagnosis and sex, and the adjusted HR value was assessed. In agreement with the results of the Kaplan-Meier analysis, patients with *SLC20A1*[high]*ALDH1A3*[high] had the worst prognosis (Table II). Furthermore, we next examined whether driver genes mutations were associated with *ALDH1* genes expression in PDAC. As shown in Fig. S5, PDAC with *TP53* truncating mutations showed high *ALDH1A3* expression. By contrast, PDAC with *TP53* missense and truncating mutations showed low *ALDH1A1* expression.

These results suggested that *SLC20A1* was involved in cancer progression and contributed to poor clinical outcome in ALDH1A3-positive PDAC.

SLC20A1 siRNA KD in ALDH1^{high} PDAC cells suppresses tumorsphere formation and cell viability, and increases cell death and caspase-3 activity. Based on the poor prognosis of patients with *SLC20A1*[high]*ALDH1A3*[high], the current study next examined the roles of *SLC20A1* in ALDH1-positive pancreatic CSCs. As shown in Fig. S6A, both PANC-1 and MIA-PaCa-2 cell lines expressed the ALDH1A3 protein; however, ALDH1A1 protein expression was lower in PANC-1 cells. ALDH1^{high} cells derived from both PDAC cell lines exhibited CSC properties, such as self-renewal, differentiation and tumorigenesis in serial passages (PANC-1: Fig. S6B and C; MIA-PaCa-2: Fig. S6G and H), similar to our previous study on breast cancer (10). Notably, *SLC20A1* mRNA expression was enriched in ALDH1^{low} PDAC cells compared with in ALDH1^{high} PDAC cells (PANC-1: Fig. S6D; MIA-PaCa-2: Fig. S6I). Next, *in vitro* tumorsphere formation and WST-8 assays were performed. *SLC20A1* siRNA KD in ALDH1^{high} cells suppressed the tumorsphere formation and viability of both PDAC cell lines (Fig. 6A-D). These results suggested that *SLC20A1* may be required for the tumor formation and cell viability of ALDH1-positive PDAC CSCs.

To investigate the reason why *SLC20A1*-deficient ALDH1^{high} PDAC cells exhibited suppressed tumorsphere formation and cell viability, trypan blue dye exclusion and caspase-3/7 fluorometric assays were performed. It was revealed that *SLC20A1* siRNA KD in ALDH1^{high} cells significantly increased the number of trypan blue-positive cells (Fig. 6E and F). Furthermore, *SLC20A1* siRNA KD in ALDH1^{high} cells resulted in the enhancement of caspase-3 activity (Fig. 6G and H) and *SLC20A1* siRNA KD in ALDH1^{high} cells caused an increase in cell apoptosis (Fig. 6I and J). These results suggested that *SLC20A1* was involved in the survival of ALDH1-positive pancreatic CSCs via the suppression of caspase-3-dependent apoptosis.
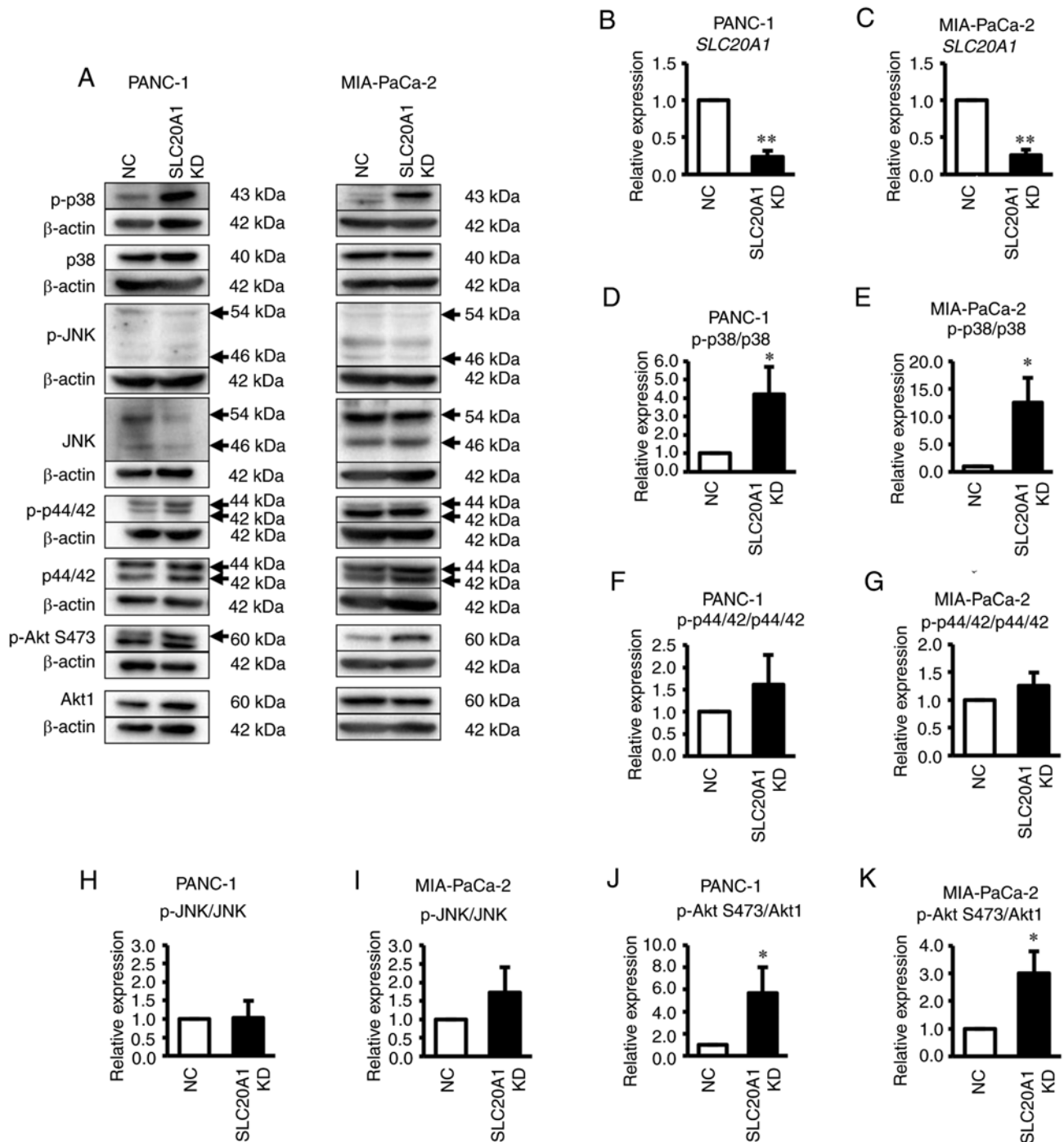
Figure 4. Western blot analysis of proteins associated with p38, JNK, p44/42 and Akt signaling following *SLC20A1* knockdown in PANC-1 and MIA-PaCa-2 cells. *SLC20A1* was knocked down in PANC-1 and MIA-PaCa-2 cells by incubation with *SLC20A1* siRNA (or NC siRNA) in a two-dimensional monolayer culture for 48 h, and the subsequent three-dimensional tumorspheres were cultured for 72 h (PANC-1) or 24 h (MIA-PaCa-2). (A) Representative western blot images. Relative *SLC20A1* mRNA expression following transfection with *SLC20A1* siRNA or NC siRNA in (B) PANC-1 and (C) MIA-PACA-2 cells. Levels of p-p38 in (D) PANC-1 and (E) MIA-PaCa-2 cells. Levels of p-p44/42 in (F) PANC-1 and (G) MIA-PaCa-2 cells. Level of p-JNK in (H) PANC-1 and (I) MIA-PaCa-2 cells. Level of p-AKT S473 in (J) PANC-1 and (K) MIA-PaCa-2 cells. The molecular weight of phosphorylated proteins and proteins is shown on the right of the blot images. (D-K) Evaluation of the ratio of phosphorylated protein/total protein. $^*P < 0.05$, $^{**}P < 0.01$ vs. NC; unpaired Student's t-test. *SLC20A1*, solute carrier family 20 member 1; siRNA, small interfering RNA; NC, negative control; KD, knockdown; p-, phosphorylated.

Discussion

The present study revealed that patients with *SLC20A1*high in PDAC had a poorer prognosis than patients with *SLC20A1*low, particularly at the early tumor stages. Moreover, patients with *SLC20A1*high*ALDH1A3*high PDAC had the poorest prognosis, and *SLC20A1* was observed to be involved in the tumorsphere

formation and cell survival of ALDH1-positive PDAC CSCs. Thus, *SLC20A1* may be used as a prognostic marker and new therapeutic target of ALDH1-positive pancreatic CSCs.

Several genes, including *SLC20A1*, have been reported as PDAC prognostic score by the analysis of OS (25,26). The present survival analyses based on DSS, DFI and PFI in PDAC were consistent with previous reports (Fig. 1;
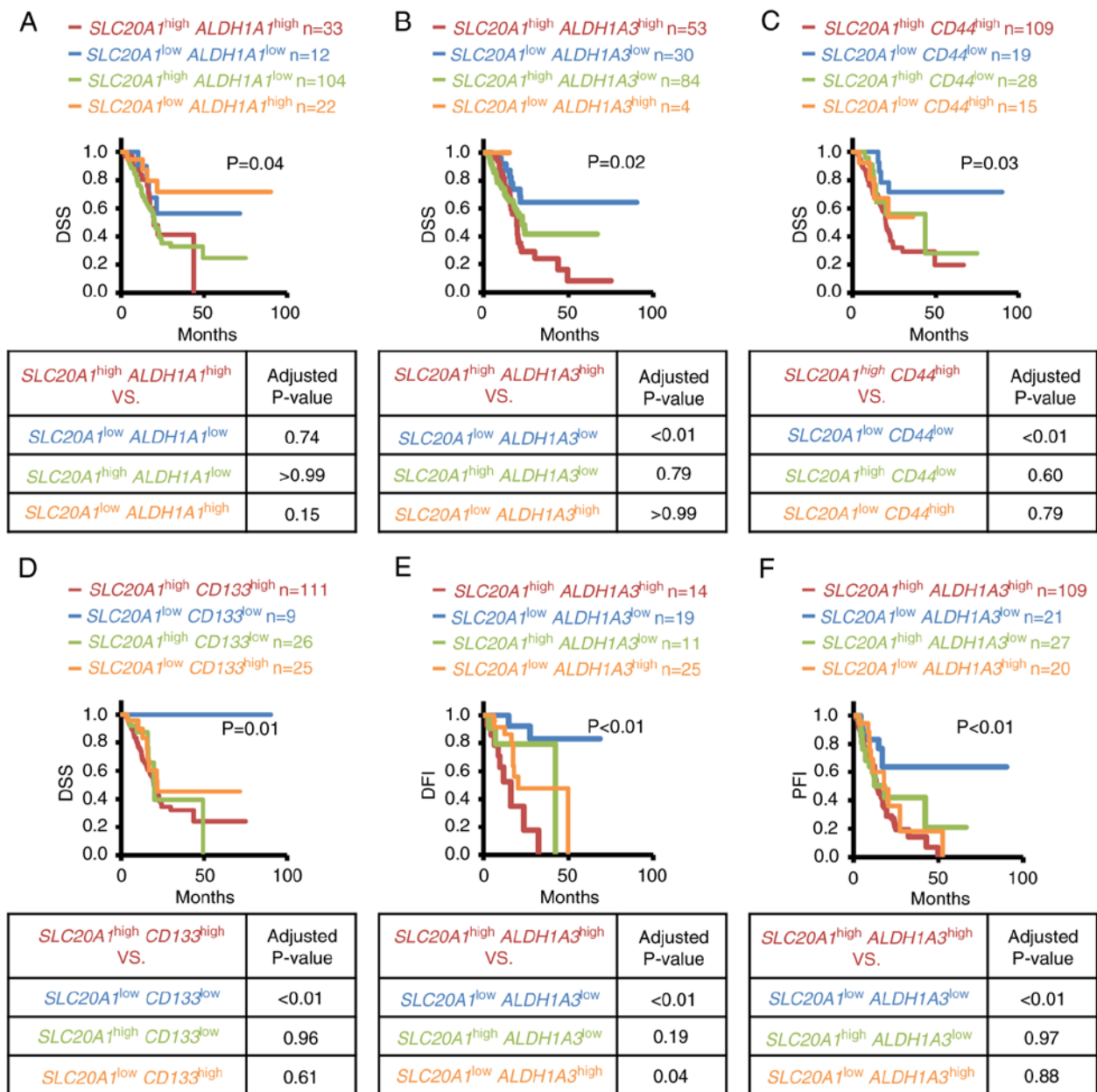
Figure 5. Kaplan-Meier analyses of the *SLC20A1*high CSC marker high, *SLC20A1*low CSC marker low, *SLC20A1*high CSC marker low and *SLC20A1*low CSC marker high groups of patients with pancreatic cancer. The Cancer Genome Atlas Pan-Cancer data were downloaded from cBioPortal. (A-D) Comparison of DSS. Adjusted P-values were determined for *SLC20A1*high CSC marker high vs. *SLC20A1*low CSC marker low, *SLC20A1*high CSC marker low or *SLC20A1*low CSC marker high groups using the Bonferroni method. (A) *ALDH1A1*, (B) *ALDH1A3*, (C) *CD44* and (D) *CD133*. (E and F) Kaplan-Meier analyses of (E) DFI and (F) PFI among *SLC20A1*high *ALDH1A3*high, *SLC20A1*low *ALDH1A3*low, *SLC20A1*high *ALDH1A3*low and *SLC20A1*low *ALDH1A3*high groups of patients. Adjusted P-values were determined for *SLC20A1*high *ALDH1A3*high vs. *SLC20A1*low *ALDH1A3*low, *SLC20A1*high *ALDH1A3*low or *SLC20A1*low *ALDH1A3*high groups using the Bonferroni method. (E) DFI and (F) PFI. *SLC20A1*high CSC marker high, patients with high expression of *SLC20A1* and CSC marker; *SLC20A1*low CSC marker low, patients with low expression of *SLC20A1* and CSC marker; *SLC20A1*high CSC marker low, patients with high expression of *SLC20A1* and low expression of CSC marker; *SLC20A1*low CSC marker high, patients with low expression of *SLC20A1* and high expression of CSC marker; DSS, disease-specific survival; DFI, disease-free interval; PFI, progression-free interval; *SLC20A1*, solute carrier family 20 member 1; CSC, cancer stem cell; *ALDH1A1*, aldehyde dehydrogenase 1 family member A1; *ALDH1A3*, aldehyde dehydrogenase 1 family member A3; *CD44*, *CD44* molecule; *CD133*, prominin 1.

Table I) (27,28). Notably, the present results revealed that patients with *SLC20A1*high showed a poorer prognosis than patients with *SLC20A1*low at tumor stage I. In PDAC, early recurrence after resection is a serious problem, even though the lesion may be found at resectable states (3-5). In breast cancer, patients with *SLC20A1*high have also been reported to exhibit a poorer prognosis than patients with *SLC20A1*low at stage I (22). Furthermore, patients with *SLC20A1*high luminal A and B breast cancer have a higher risk of

recurrence >10 years later after endocrine therapy (22). In PDAC, however, *SLC20A1*high tumors progress in a short interval of time after medical treatment. Furthermore, high *SLC20A1* gene expression may be associated with *KRAS* missense and truncating mutations, and deep deletion and deletion of *CDKN2A*, *TP53* and *SMAD4*, which are introduced during the premalignant progression of PDAC. Thus, *SLC20A1* could contribute to the aggressive progression of PDAC from an early stage.
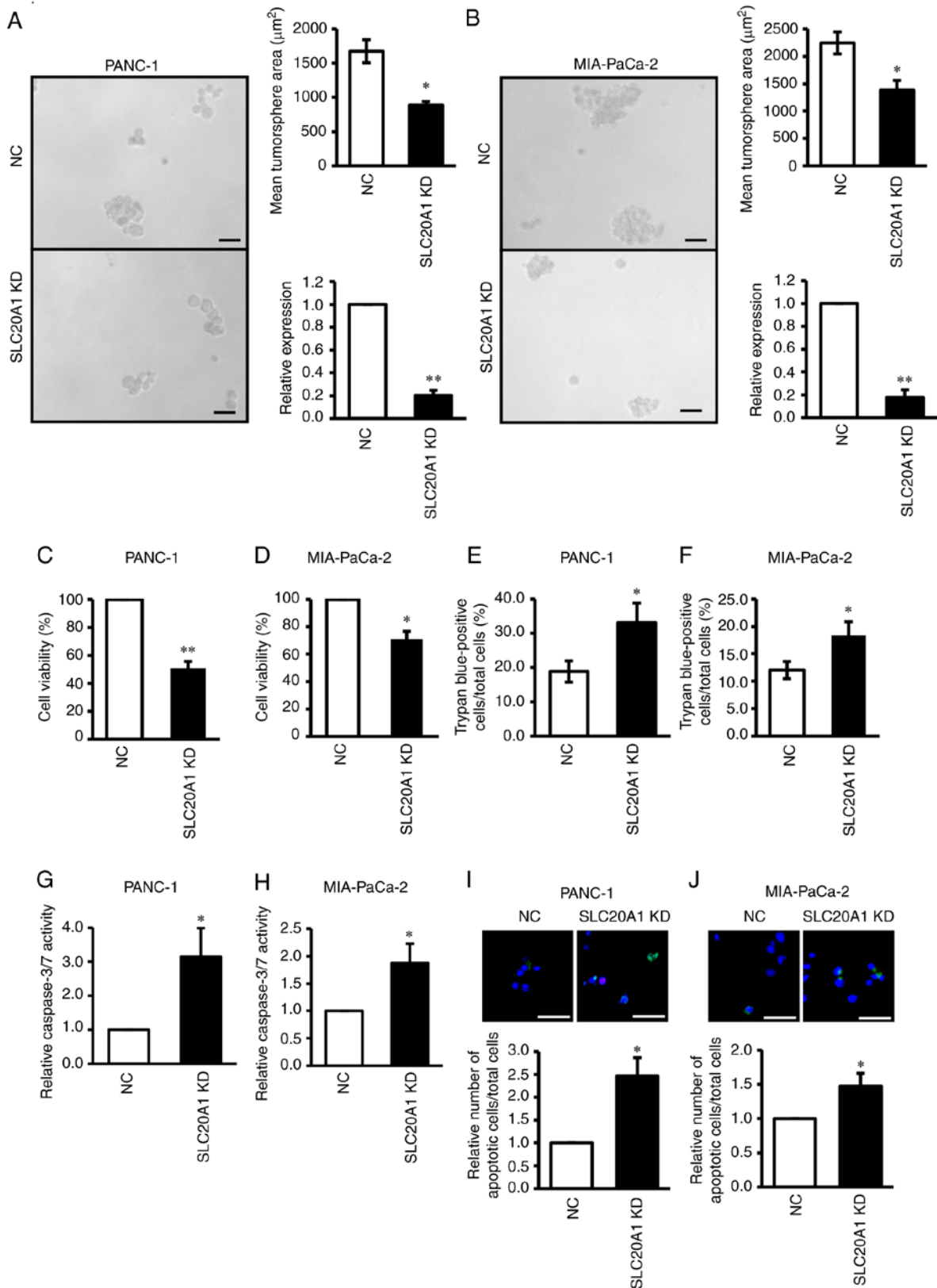
Figure 6. Effects of *SLC20A1* small interfering RNA KD on the tumorsphere formation, viability, cell death and apoptosis of ALDH1^{high} pancreatic cancer cells. Representative images, mean tumorsphere area and relative *SLC20A1* mRNA expression following transfection with *SLC20A1* siRNA or NC siRNA in (A) PANC-1 and (B) MIA-PaCa-2 ALDH1^{high} cells. Scale bar, 50 μm. Viability of (C) PANC-1 and (D) MIA-PaCa-2 ALDH1^{high} cells was assessed using 5-{2,4-bis[(sodiooxy)sulfonyl]phenyl}-2-(2-methoxy-4-nitrophenyl)-3-(4-nitrophenyl)-3H-1,2λ5,3,4-tetrazol-2-ylium assays. Trypan blue-positive (E) PANC-1 and (F) MIA-PaCa-2 ALDH1^{high} cells. The total cells and the stained cells were counted using a hematocytometer and the percentage of the stained cells per total cells was calculated. Relative caspase-3/7 activity of (G) PANC-1 and (H) MIA-PaCa-2 ALDH1^{high} cells, as assessed by a caspase-3/7 fluorometric assay. Apoptotic cell staining and relative apoptosis of (I) PANC-1 and (J) MIA-PaCa-2 ALDH1^{high} cells. Representative immunofluorescence staining of Apopxin™ Green (green), 7-amino-actinomycin D (red) and Hoechst 33342 staining (blue). Scale bar, 50 μm. *$P<0.05$, **$P<0.01$ vs. NC; unpaired Student's t-test. ALDH1high, high ALDH1 activity; *SLC20A1*, solute carrier family 20 member 1; KD, knockdown; NC, negative control; ALDH1, aldehyde dehydrogenase 1; siRNA, small interfering RNA.

SLC20A1 has previously been shown to be involved in cell proliferation in pre-osteoblastic MC3T3-E1 and NIH3T3 cells (33,34). SLC20A1 depletion causes an increase in TNF-dependent p38 MAPK activation, a delay in entry to the G_2/M phase in HeLa cells (32,33), and TNF-induced caspase-3-dependent apoptosis via the JNK signaling pathway in HeLa cells (32). The current study also revealed that *SLC20A1* depletion caused p38 phosphorylation, caspase-3 activation and increased cell death in PDAC cells. Thus, *SLC20A1* may be involved in cell survival via the suppression of caspase-dependent apoptosis. The SLC20A1 protein mediates the uptake of Pi into cells (20,21). Notably, Pi uptake is not affected by SLC20A1-depletion (50) and SLC20A1 overexpression in MC3T3-E1 cells does not affect Pi uptake (34). Furthermore, the introduction of Pi-uptake defective SLC20A1 (S128A) into SLC20A1-deficient cells has been shown to restore cell viability (33). Thus, SLC20A1 may be involved in the regulation of Pi uptake-dependent and -independent cell survival. The detailed mechanism underlying the SLC20A1-dependent regulation of cell survival remains to be elucidated. ALDH1A1 is used as a CSC marker in PDAC (14,15). The present study revealed that ALDH1^{high} cells concentrated ALDH1-positive CSCs in MIA-PaCa-2 and PANC-1 cells. As shown in Fig. S6A, although ALDH1A3 was highly expressed in both MIA-PaCa-2 and PANC-1 cells, ALDH1A1 exhibited less expression in PANC-1 cells. These results suggested that *ALDH1A3* may be a major gene of the ALDH1 family contributing to ALDH1 activity in PDAC cells, as well as in breast cancer (44,51). As aforementioned, although *SLC20A1* has been reported as a gene of PDAC prognostic score (25,26), *ALDH1A3* is not included in the PDAC prognostic score. The present results suggested that ALDH1A3 is also an important factor in predicting the prognosis of PDAC. Notably, ALDH1A3 has been reported to be a prognostic factor for various types of cancers (10,16,17,40,44). Both *SLC20A1*[high]*ALDH1A1*[high] and *SLC20A1*[high]*ALDH1A1*[low] also have poor prognoses. *SLC20A1* may function in cells positive for cancer stem cell markers other than ALDH1A3. In fact, as shown in Fig. S2, *SLC20A1* gene expression is correlated with the expression of other stem cell-related genes, such as *CD44*, in addition to *ALDH1A3*. However, as shown in Figs. 1 and S5, *SLC20A1* and *ALDH1A3* gene expression levels were associated with *TP53* mutation. Other than that, *ALDH1A1* gene expression was inversely associated with *KRAS* missense mutations and *TP53* mutation. In addition, as shown in Fig. S2, although the *SLC20A1* gene is correlated with the *ALDH1A3* gene, *SLC20A1* gene is inversely correlated with the *ALDH1A1* gene. Thus, the *SLC20A1* gene, but not the *ALDH1A1* gene, plays an important function in ALDH1A3-positive cells.

SLC20A1 siRNA KD suppressed *in vitro* tumorsphere formation, cell viability, p38 activation, caspase-3 activity and cell death in ALDH1^{high} PDAC cells. Notably, although *SLC20A1* is enriched in ALDH1^{low} cells rather than ALDH1^{high} cells, ALDH1^{high} PDAC cells exhibited tumorsphere forming ability, whereas ALDH1^{low} PDAC cells did not. These results suggested that *SLC20A1* was involved in the survival of ALDH1-positive pancreatic CSCs by suppressing caspase-3-dependent apoptosis. SLC20A1 is required for cell proliferation, whereas the phosphate transport activity is independent of cell proliferation (33). Thus, *SLC20A1* in ALDH1^{low}

cells may contribute to functions other than cell proliferation. Our previous report showed that *SLC20A1* also contributes to the *in vitro* tumorsphere formation and cell viability of ALDH1-positive breast CSCs (23). ALDH1 is known as a CSC marker in multiple cancer types (9-16,18). Therefore, these results suggested that *SLC20A1* may be involved in the stemness of ALDH1-positive CSCs, and may act as a prognostic marker and therapeutic target in various types of cancer types. In the present study, we only showed the experimental results for loss-of-function of *SLC20A1*. Although we examined the effect of transient and stable overexpression of *SLC20A1* in response to an expression vector in pancreatic cell lines, the results were inconsistent and precise results could not be obtained. Therefore, the validation of our findings in the experiments for gain-of-function of *SLC20A1* will be needed. In the present study, we revealed the role of *SLC20A1* in PDAC stem cells via *in vitro* experiments, and by analyzing a public dataset including data on gene mutations, gene expression, and clinical information. It will be important to validate these results via immunohistochemical analysis of patient samples and analysis of PDAC model mice in the future.

In conclusion, the present study indicated that *SLC20A1* is involved in the tumorsphere formation and cell survival of ALDH1-positive pancreatic CSCs, and contributes to cancer progression and poor clinical outcome in PDAC. Therefore, *SLC20A1* may be used as a prognostic biomarker and new therapeutic target for ALDH1-positive pancreatic CSCs.

Availability of data and materials

The data generated in the present study may be requested from the corresponding author.

Authors' contributions

IM, TK, CO and YH performed the experiments. IM, TK, CO, ST and KA confirmed the authenticity of all the raw data. IM, TK, CO, YM, YT, HaM, ST, AO and HiM performed the

bioinformatics analysis. IM, TK, CO, ST, AO, HiM, YM, YT, HaM, YX, KeS, KaS and SO contributed to interpretation of data. IM, TK, CO and KA conceived the study. IM, TK, CO, AO, HiM, YM, YT, HaM and KA drafted the manuscript. IM, TK, CO, ST, AO, HiM, YM, YT, HaM, KaS, SO and KA contributed to discussion and review of the manuscript. All authors have read and approved the final version of the manuscript.

Ethics approval and consent to participate

Not applicable.

Patient consent for publication

Not applicable.

Competing interests

The authors declare that they have no competing interests.

References

1. Sung H, Ferlay J, Siegel RL, Laversanne M, Soerjomataram I, Jemal A and Bray F: Global cancer statistics 2020:GLOBOCAN estimates of incidence and mortality worldwide for 36 cancers in 185 countries. CA Cancer J Clin 71: 209-249, 2021.
2. Siegel RL, Miller KD, Wagle NS and Jemal A: Cancer statistics, 2023. CA Cancer J Clin 73: 17-48, 2023.
3. McGuigan A, Kelly P, Turkington RC, Jones C, Coleman HG and McCain RS: Pancreatic cancer: A review of clinical diagnosis, epidemiology, treatment and outcomes. World J Gastroenterol 24: 4846-4861, 2018.
4. Grant TJ, Hua K and Singh A: Molecular pathogenesis of pancreatic cancer. Prog Mol Biol Transl Sci 144: 241-275, 2016.
5. Kern SE, Hruban RH, Hidalgo M and Yeo CJ: An introduction to pancreatic adenocarcinoma genetics, pathology and therapy. Cancer Biol Ther 1: 607-613, 2002.
6. Reya T, Morrison SJ, Clarke MF and Weissman IL: Stem cells, cancer, and cancer stem cells. Nature 414: 105-111, 2001.
7. Visvader JE and Lindeman GJ: Cancer stem cells: Current status and evolving complexities. Cell Stem Cell 10: 717-728, 2012.
8. Diehn M, Cho RW, Lobo NA, Kalisky T, Dorie MJ, Kulp AN, Qian D, Lam JS, Ailles LE, Wong M, et al: Association of reactive oxygen species levels and radioresistance in cancer stem cells. Nature 458: 780-783, 2009.
9. Ginestier C, Hur MH, Charafe-Jauffret E, Monville F, Dutcher J, Brown M, Jacquemier J, Viens P, Kleer CG, Liu S, et al: ALDH1 is a marker of normal and malignant human mammary stem cells and a predictor of poor clinical outcome. Cell Stem Cell 1: 555-567, 2007.
10. Nozaki Y, Tamori S, Inada M, Katayama R, Nakane H, Minamishima O, Onodera Y, Abe M, Shiina S, Tamura K, et al: Correlation between c-Met and ALDH1 contributes to the survival and tumor-sphere formation of ALDH1 positive breast cancer stem cells and predicts poor clinical outcome in breast cancer. Genes Cancer 8: 628-639, 2017.
11. Kim MP, Fleming JB, Wang H, Abbruzzese JL, Choi W, Kopetz S, McConkey DJ, Evans DB and Gallick GE: ALDH activity selectively defines an enhanced tumor-initiating cell population relative to CD133 expression in human pancreatic adenocarcinoma. PLoS One 6: e20636, 2011.
12. Rasheed ZA, Yang J, Wang Q, Kowalski J, Freed I, Murter C, Hong SM, Koorstra JB, Rajeshkumar NV, He X, et al: Prognostic significance of tumorigenic cells with mesenchymal features in pancreatic adenocarcinoma. J Natl Cancer Inst 102: 340-351, 2010.
13. Kim SK, Kim H, Lee DH, Kim TS, Kim T, Chung C, Koh GY, Kim H and Lim DS: Reversing the intractable nature of pancreatic cancer by selectively targeting ALDH-high, therapy-resistant cancer cells. PLoS One 8: e78130, 2013.
14. Marcato P, Dean CA, Giacomantonio CA and Lee PWK: Aldehyde dehydrogenase: Its role as a cancer stem cell markaer comes down to the specific isoform. Cell Cycle 10: 1378-1384, 2011.
15. Shingh S, Arcaroli J, Thompson DC, Messersmith W and Vasiliou V: Acetaldehyde and retinaldehyde-metabolizing enzymes in colon and pancreatic cancers. Adv Exp Med Biol 815: 281-294, 2015.
16. McLean ME, McLean MR, Cahill HF, Arun RP, Walker OL, Wasson MCD, Fernando W, Venkatesh J and Marcato P: The expanding role of cancer stem cell marker ALDH1A3 in cancer and beyond. Cancers (Basel) 15: 492, 2023.
17. Kasai T, Tamori S, Takasaki Y, Matsuoka I, Ozaki A, Matsuda C, Harada Y, Sasaki K, Ohno S and Akimoto K: High expression of PKCλ and ALDH1A3 indicates a poor prognosis, and PKCλ is required for the asymmetric cell division of ALDH1A3-positive cancer stem cells in PDAC. Biochem Biophys Res Commun 669: 85-94, 2023.
18. Jia J, Parikh H, Xiao W, Hoskins JW, Pflicke H, Liu X, Collins I, Zhou W, Wang Z, Powell J, et al: An integrated transcriptome and epigenome analysis identifies a novel candidate gene for pancreatic cancer. BMC Medical Genom 6: 33, 2013.
19. Nie S, Qian X, Shi M, Li H, Peng C, Ding X, Zhang S, Zhang B, Xu G, Lv Y, et al: ALDH1A3 accelerates pancreatic cancer metastasis by promoting glucose metabolism. Flont Oncol 10: 915, 2020.
20. Johann SV, Gibbons JJ and O'Hara B: GLVR1, a receptor for gibbon ape leukemia virus, is homologous to a phosphate permease of Neurospora crassa and is expressed at high levels in the brain and thymus. J Virol 66: 1635-1640, 1992.
21. Kavanaugh MP, Miller DG, Zhang W, Law W, Kozak SL, Kabat D and Miller AD: Cell-surface receptors for gibbon ape leukemia virus and amphotropic murine retrovirus are inducible sodium-dependent phosphate symporters. Proc Natl Acad Sci USA 91: 7071-7075, 1994.
22. Onaga C, Tamori S, Matsuoka I, Ozaki A, Motomura H, Nagashima Y, Sato T, Sato K, Xiong Y, Sasaki K, et al: High expression of SLC20A1 is less effective for endocrine therapy and predicts late recurrence in ER-positive breast cancer. PLoS One 17: e0268799, 2022.
23. Onaga C, Tamori S, Motomura H, Ozaki A, Matsuda C, Matsuoka I, Fujita T, Nozaki Y, Hara Y, Kawano Y, et al: High SLC20A1 expression is associated with poor prognoses in claudin-low and basal-like breast cancers. Anticancer Res 41: 43-54, 2021.
24. Onaga C, Tamori S, Matsuoka I, Ozaki A, Motomura H, Nagashima Y, Sato T, Sato K, Tahata K, Xiong Y, et al: High SLC20A1 expression is associated with poor prognosis for radiotherapy of estrogen receptor-positive breast cancer. Cancer Diagn Progn 2: 429-442, 2022.
25. Haider S, Wang J, Nagano A, Desai A, Arumugam P, Dumartin L, Fitzgibbon J, Hagemann T, Marshall JF, Kocher HM, et al: A multi-gene signature predicts outcome in patients with pancreatic ductal adenocarcinoma. Genome Med 6: 105, 2014.
26. Canlı SD, Dedeoğlu E, Akbar MW, Küçükkaraduman B, İşbilen M, Erdoğan ÖŞ, Erciyas SK, Yazıcı H, Vural B and Güre AO: A novel 20-gene prognostic score in pancreatic adenocarcinoma. PLoS One 15: e0231835, 2020.
27. Ouyang J, Hu Z, Tong J, Yang Y, Wang J, Chen X, Luo T, Yu S, Wang X and Huang S: Construction and evaluation of a nomogram for predicting survival in patients with lung cancer. Aging (Albany NY) 14: 2775-2792, 2022.
28. Okamoto T, Onaga C, Matsuoka I, Ozaki A, Matsuda C, Kasai T, Xiong Y, Harada Y, Sato T, Nakano Y, et al: High SLC20A1 expression indicates poor prognosis in prostate cancer. Cancer Diagn Progn 3: 439-448, 2023.
29. Sato K and Akimoto K. Expression levels of KMT2C and SLC20A1 identified by information-theoretical analysis are powerful prognostic biomarkers in estrogen receptor-positive breast cancer. Clin Breast Cancer 17: e135-e142, 2017.
30. Shen T, Wang M and Wang X: Identification of prognosis-related Hub RNA binding proteins function through regulating metabolic processes in tongue cancer. J Cancer 12: 2230-2242, 2021.
31. Dong Z, Wang J, Zhan T and Xu S: Identification of prognostic risk factors for esophageal adenocarcinoma using bioinformatics analysis. Onco Targets Ther 11: 4327-4337, 2018.
32. Salaün C, Leroy C, Rousseau A, Boitez V, Beck L and Friedlander G: Identification of a novel transport-independent function of PiT1/SLC20A1 in the regulation of TNF-induced apoptosis. J Biol Chem 285: 34408-34418, 2010.
33. Beck L, Leroy C, Salaün C, Margall-Ducos G, Desdouets C and Friedlander G: Identification of a novel function of PiT1 critical for cell proliferation and independent of its phosphate transport activity. J Biol Chem 284: 31363-31374, 2009.

34. Byskov K, Jensen N, Kongsfelt IB, Wielsøe M, Pedersen LE, Haldrup C and Pedersen L: Regulation of cell proliferation and cell density by the inorganic phosphate transporter PiT1. Cell Div 7: 7, 2012.

35. Cancer Genome Atlas Research Network; Weinstein JN, Collisson EA, Mills GB, Shaw KR, Ozenberger BA, Ellrott K, Shmulevich I, Sander C and Stuart JM: The cancer genome atlas pan-cancer analysis project. Nat Genet 45: 1113-1120, 2013.

36. Hoadley KA, Yau C, Hinoue T, Wolf DM, Lazar AJ, Drill E, Shen R, Taylor AM, Cherniack AD, Thorsson V, *et al*: Cell-of-origin patterns dominate the molecular classification of 10,000 tumors from 33 types of cancer. Cell 173: 291-304, 2018.

37. Cerami E, Gao J, Dogrusoz U, Gross BE, Sumer SO, Aksoy BA, Jacobsen A, Byrne CJ, Heuer ML, Larsson E, *et al*: The cBio cancer genomics portal: an open platform for exploring multidimensional cancer genomics data. Cancer Discov 2: 401-404, 2012.

38. Gao J, Aksoy BA, Dogrusoz U, Dresdner G, Gross B, Sumer SO, Sun Y, Jacobsen A, Sinha R, Larssson E, *et al*: Integrative analysis of complex cancer genomics and clinical profiles using the cBioPortal. Sci Signal 6: pl1, 2013.

39. Chandrashekar DS, Bashel B, Balasubramanya SAH, Creighton CJ, Ponce-Rodriguez I, Chakravarthi BVSK and Varambally S: UALCAN: A portal for facilitating tumor subgroup gene expression and survival analyses. Neoplasia 19: 649-658, 2017.

40. Nozaki Y, Motomura H, Tamori S, Kimura Y, Onaga C, Kanai S, Ishihara Y, Ozaki A, Hara Y, Harada Y, *et al*: High PKCλ expression is required for ALDH1-positive cancer stem cell function and indicates a poor clinical outcome in late-stage breast cancer patients. PLoS One 15: e0235747 2020.

41. Motomura H, Tamori S, Yatani MK, Namiki A, Onaga C, Ozaki A, Takasawa R, Mano Y, Sato T, Hara Y, *et al*: GLO 1 and PKCλ regulate ALDH1-positive breast cancer stem cell survival. Anticancer Res 41: 5959-5971, 2021.

42. Ozaki A, Motomura H, Tamori S, Onaga C, Nagashima Y, Kotori M, Matsuda C, Matsuda A, Mochizuki N, Sato T, *et al*: High expression of p62 and ALDH1A3 is associated with poor prognosis in luminal b breast cancer. Anticancer Res 42: 3299-3312, 2022.

43. Xiong Y, Motomura H, Tamori S, Ozaki A, Onaga C, Hara Y, Sato K, Tahata K, Harada Y, Sasaki K, *et al*: High expression of CD58 and ALDH1A3 predicts a poor prognosis in basal-like breast cancer. Anticancer Res 42: 5223-5232, 2022.

44. Tamori S, Nozaki Y, Motomura H, Nakane H, Katayama R, Onaga C, Kikuchi E, Shimada N, Suzuki Y, Noike M, *et al*: Glyoxalase 1 gene is highly expressed in basal-like human breast cancers and contributes to survival of ALDH1-positive breast cancer stem cells. Oncotarget 9: 36515-36529, 2018.

45. Motomura H, Ozaki A, Tamori S, Onaga C, Nozaki Y, Waki Y, Takasawa R, Yoshizawa K, Mano Y, Sato T, *et al*: Glyoxalase 1 and protein kinase Cλ as potential therapeutic targets for late-stage breast cancer. Oncol Lett 22: 547, 2021.

46. Connor AA and Gallinger S: Pancreatic cancer evolution and heterogeneity: Integrating omics and clinical data. Nat Rev Cancer 22: 131-142, 2022.

47. Hong SP, Wen J, Bang S, Park S and Song SY: CD44-positive cells are responsible for gemcitabine resistance in pancreatic cancer cells. Int J Cancer 125: 2323-2331, 2009.

48. Hermann PC, Huber SL, Herrler T, Aicher A, Ellwart JW, Guba M, Bruns CJ and Heeschen C: Distinct populations of cancer stem cells determine tumor growth and metastatic activity in human pancreatic cancer. Cell Stem Cell 1: 313-323, 2007.

49. Maeda S, Shinchi H, Kurahara H, Mataki Y, Maemura K, Sato M, Natsugoe S, Aikou T and Takao S: CD133 expression is correlated with lymph node metastasis and vascular endothelial growth factor-C expression in pancreatic cancer. Br J Cancer 98: 1389-1397, 2008.

50. Beck L, Leroy C, Cormier SB, Forand A, Salaün C, Paris N, Bernier A, Ureña-Torres P, Prié D, Ollero M, *et al*: The phosphate transporter PiT1 (Slc20a1) revealed as a new essential gene for mouse liver development. PLoS One 5: e9148, 2010.

51. Marcato P, Dean CA, Liu RZ, Coyle KM, Bydoun M, Wallace M, Clements D, Turner C, Mathenge EG, Gujar SA, *et al*: Aldehyde dehydrogenase 1A3 influences breast cancer progression via differential retinoic acid signaling. Mol Oncol 9: 17-31, 2015.